Thermal and Mechanical Behavior of Polyamide 6/ Polyamide 6I/6T Blends

A. SICILIANO,[1,*] D. SEVERGNINI,[1] A. SEVES,[1] T. PEDRELLI,[2] and L. VICINI[2]

[1]Stazione Sperimentale per la Cellulosa, Carta e Fibre Tessili Vegetali ed Artificiali, Piazza Leonardo da Vinci 26, 20133 Milan, Italy; [2]Stazione Sperimentale per l'Industria delle Conserve Alimentari. Viale Tanara 33, 43100 Parma, Italy

SYNOPSIS

The thermal and mechanical properties of blends, obtained by mixing polyamide 6 (PA6) and an amorphous aromatic copolyamide G21 (ISO nomenclature PA 6I/6T), were investigated by differential scanning calorimetry, dynamic mechanical analysis, and mechanical tensile tests. Quenched blends show a single glass transition temperature; the T_g-composition trend was interpreted by means of the Gordon–Taylor equation. The half-time of crystallization decreases by increasing the G21 content and this indicates a depression of the overall crystallization rate. A small decrease in the equilibrium melting temperature of PA6 in the blends was observed; this finding suggests that the interaction parameter in PA6/G21 blends is probably very small. The dynamic mechanical analysis of crystallized blends suggests the presence of a homogeneous amorphous phase even if the crystallization of PA6 occurred. The tensile mechanical properties reveal that G21 acts as stiffener of PA6. The collected experimental data suggest that PA6 and G21 are miscible in the composition range investigated. © 1996 John Wiley & Sons, Inc.

INTRODUCTION

Polyamide 6 (PA6) films show good performances such as chemical and mechanical resistance, barrier properties to gas and aromas, thermoforming and shrink properties, transparency, and printability. Due to these peculiarities, PA6 film is widely used in medical and food packaging.

A great increase of the applications is expected when PA6 is modified by adding a second component to improve some properties. G21 (ISO nomenclature PA 6I/6T) is an amorphous aromatic copolyamide obtained from the condensation of examethylenediamine with terephthalic and isophthalic acids, whose structural formula is

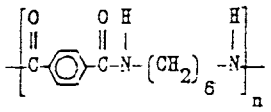

G21 has good mechanical and gas barrier properties; moreover, in contrast to polyamide 6, the barrier properties improve with increasing relative humidity.[1,2]

In a recent series of articles, Ellis extensively studied the phase behavior of polyamide-based blends.[3-8] These works pointed out the existence of simple relationships between structure and miscibility that are explained by a theory based upon a binary interaction model.[9] An estimation of the Flory interaction parameter (X_{blend}) for various aliphatic/aromatic polyamide blends was performed; in particular, for a system composed of PA6 and an aromatic copolyamide with the same structure as that of G21, an X_{blend} value of -0.0104,[4] suggesting the existence of a favorable interaction between the components, was found. The aim of the present work was to investigate the thermal and mechanical properties of PA6/G21 blends.

EXPERIMENTAL

Materials and Specimen Preparation

The polymers used in this work were a general-purpose nylon 6 (F34 GRILON, M_n = 26,000) and an

* To whom correspondence should be addressed.

Journal of Applied Polymer Science, Vol. 60, 1757–1764 (1996)
 CCC 0021-8995/96/101757-08

amorphous copolyamide (GRIVORY G21); both the polymers were supplied by EMS Chemie (CH). The composition of G21 was analyzed using a nuclear magnetic resonance (NMR) method[4]; the molar ratio of the isophtalic/terephtalic acid isomers was found to be 2.06. The viscosity number of G21 in a dilute solution is 19 dL/g (NF T 51-019).

Blends of PA6 and G21 with weight ratios of 100/0, 90/10, 80/20, 70/30, 60/40, 50/50, 30/70, and 0/100 were prepared by melt-mixing in a Gimac single-screw extruder. The pellets of PA6 and G21 were frozen in liquid nitrogen and finely ground; the powders obtained were mixed in the appropriate ratios and put on the extruder hopper, this procedure allows one to obtain a good physical mixture of the two components. The screw speed was adjusted to 30 rpm and the die temperature was 240°C. Both PA6 and G21 were not significantly degraded after the grounding and extrusion processes.

Samples in the form of strips were obtained using two water-cooled rolls. Individual specimens (5 mm in width) were cut from the strips (0.5 mm in thickness) using a razor blade. For the mechanical tests, the specimens were previously treated for 20 min at 120°C to promote the full crystallization of PA6.

Morphology

The morphology of PA6 spherulites was studied by an optical polarizing microscope equipped with a Mettler automatic hot stage; the blends were melted at 260°C for 30 min and isothermally crystallized at 194°C.

Thermal Properties

The thermal properties and the isothermal kinetics of crystallization were studied by differential scanning calorimetry (Perkin-Elmer DSC-4 calorimeter equipped with an intercooler system). To determine the crystallization (T_c) and the melting (T_m) temperatures, the samples were melted at 260°C for 2 min, then cooled down to −50°C (crystallization run), and, finally, heated up to 250°C (melting run).

Quench-cooled samples were obtained by plunging the blends melted at 260°C for 2 min into liquid nitrogen. The samples were scanned from −50 to 260°C; the glass transition temperature (T_g), the cold-crystallization (T_{cc}), and melting (T_m) temperatures were obtained from DSC plots. A scan rate of 20°C/min was used throughout.

The T_g values were taken as the temperature corresponding to the maximum of the peak of the first-order derivative of the transition traces. The melting and the crystallization temperatures were taken as the peak temperature of the melting endotherm and the crystallization exotherm, respectively.

Isothermal Crystallization Kinetics

To study the isothermal crystallization kinetics of the 100/0, 90/10, 80/20, 70/30, and 60/40 blends, the samples were melted for 30 min at 260°C to destroy the "crystalline memory" of PA6[10] and then rapidly cooled to the desired crystallization temperature (T_c). The heat evolved during the isothermal crystallization was recorded as a function of the time. The weight fraction X_t of the material crystallized at time t was calculated by the relation

$$X_t = \int_0^t \left(\frac{dH}{dt}\right) dt \Big/ \int_0^\infty \left(\frac{dH}{dt}\right) dt$$

where the first integral is the heat generated at time t and the second is the total heat when the crystallization is complete. The half-time of crystallization ($t_{0.5}$), defined as the time taken for half of the crystallinity to develop, was obtained.

The kinetics of isothermal crystallization were analyzed by means of the well-known Avrami equation[11]:

$$X_t = 1 - \exp(-K_n t^n)$$

where K_n is the overall kinetic rate constant and n (Avrami exponent) is a parameter that depends on the type of nucleation and on the geometry of the growing crystals. Values for K_n and n were calculated from the intercept and the slope of the straight lines obtained by plotting the quantity $\log[-\ln(1 - X_t)]$ against $\log t$. After crystallization, the samples were heated to the melting point at a scanning rate of 20°C/min; the observed melting point (T_m) and the apparent enthalpies of melting (ΔH) were obtained from the maximum and the minimum of the endothermic peaks, respectively. The crystalline weight fractions of the blends ($X_{c\text{blend}}$) and of the PA6 phase ($X_{c\text{PA6}}$) were calculated at various T_c from the ratio between ΔH and the melting enthalpy of 100% crystalline PA6 (ΔH^0 = 54.97 cal/g).[12]

Dynamic Mechanical Behavior

Dynamic mechanical measurements were performed by a dynamic mechanical analyzer (Polymer Laboratories MK III) operating in a tensile mode at a frequency of 1 Hz in the temperature range from −40 to 160°C (heating rate 3°C/min). The loss

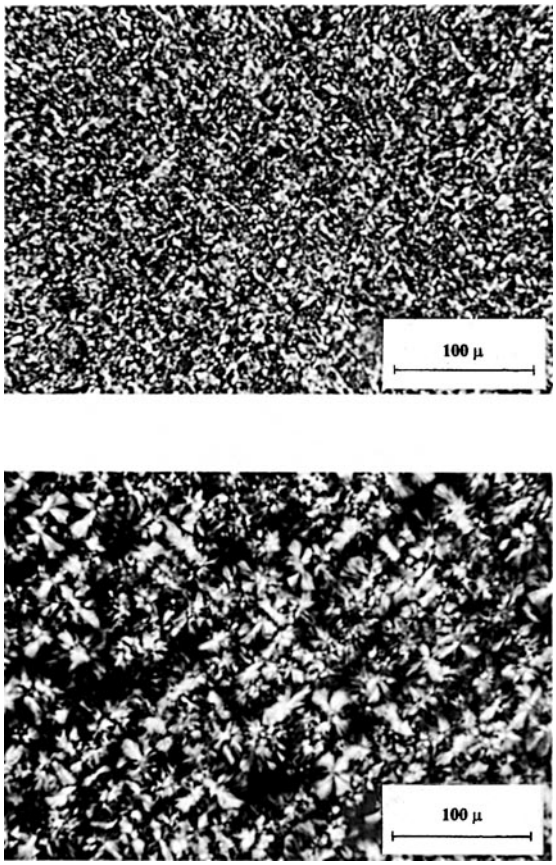

Figure 1 Optical micrographs of PA6 spherulites isothermally crystallized at 194°C: (a) PA6; (b) 60/40 blend.

modulus (E''), the storage modulus (E'), and the loss factor (tan δ) were monitored vs. temperature.

Tensile Mechanical Properties

Tensile mechanical properties were investigated by an Instron machine (Model 1122) at 23°C and RH 65%, with a crosshead speed of 50 mm/min and a gauge length of 50 mm. The Young's modulus (E), stress (σ_y), and elongation (ε_y) at yield, stress (σ_r), and elongation (ε_r) at break were calculated from stress–strain curves on an average of 10 specimens.

RESULTS AND DISCUSSION

Morphology

Optical micrographs showing PA6 and 60/40 blend spherulites are shown in Figure 1. No apparent phase separation is evident, although the very low magnification does not permit one to assert that only one amorphous phase is present. The increased

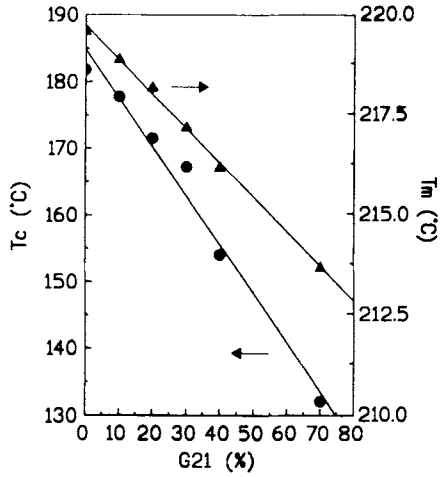

Figure 2 Crystallization (T_c) and melting (T_m) temperatures for PA6/G21 blends.

spherulite dimensions in the 60/40 blend indicate that the presence of G21 lowers the nucleation density of PA6 and reduces the radial growth rate of the spherulites, as expected for a miscible polymer system where a higher T_g amorphous component is added to a semicrystalline polymer.

Thermal Properties

After cooling from the melt, the well-known phenomenon of multiple melting peaks, due to reorganization, was not observed because of the relatively high rate of cooling employed (20°C/min). In Figure 2, the T_c and T_m values as a function of G21 content are reported; as can be seen, the T_c and T_m values

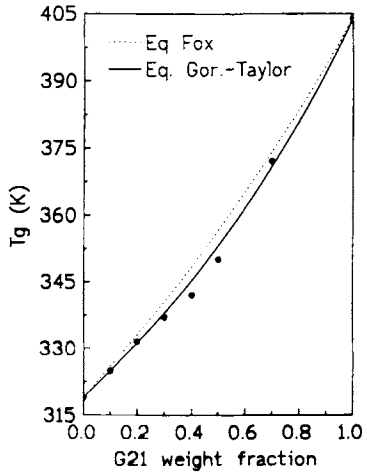

Figure 3 Glass transition temperatures for PA6/G21 blends: (●) experimental points; (· · ·) Fox equation; (——) Gordon–Taylor equation.

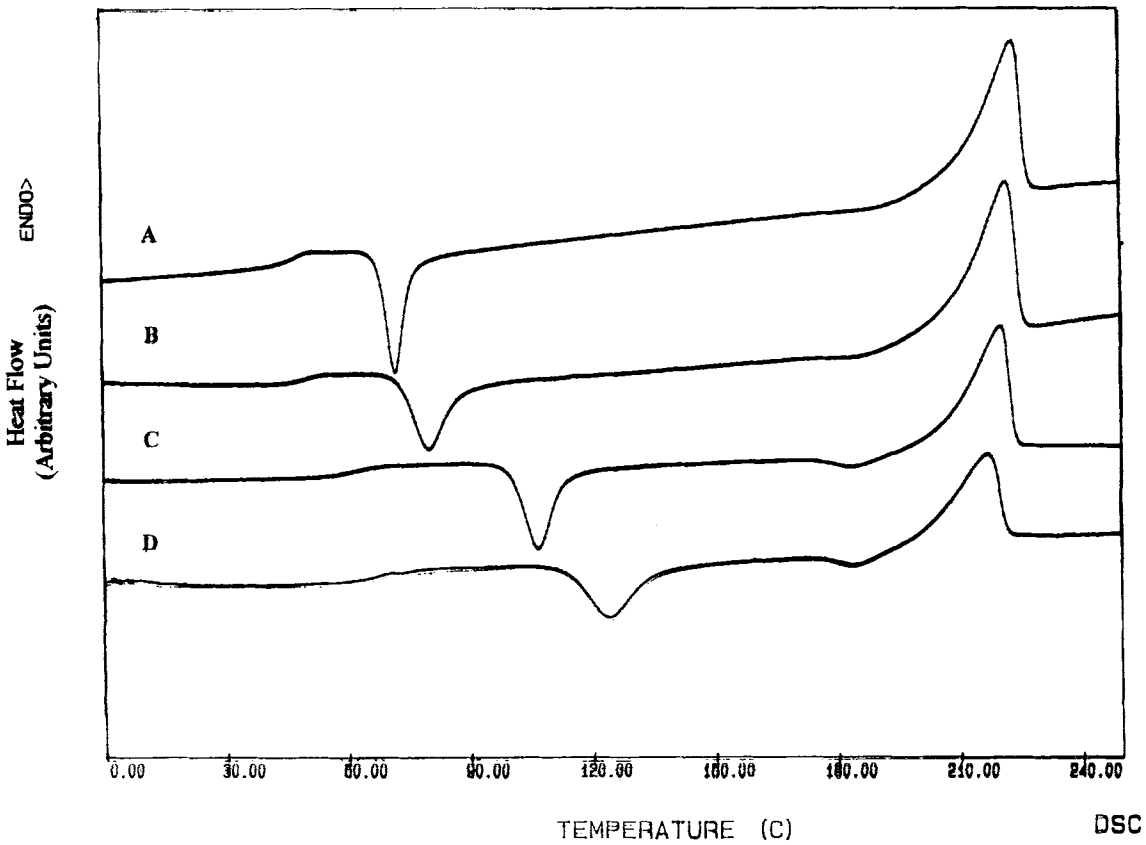

Figure 4 DSC thermograms for quench-cooled samples of (A) PA6, (B) 90/10 blend, (C) 70/30 blend, and (D) 60/40 blend.

decrease when the G21 content increases. That is expected for a system compatible in the molten state; the depression of the crystallization temperature may be ascribed to several factors[13] related to the ability of the crystallizable polymer segments to migrate to the crystallite–melt interface and to the change of composition in the melt during crystallization.

Quenched samples of PA6/G21 blends always exhibit a single T_g with a value dependent on com-

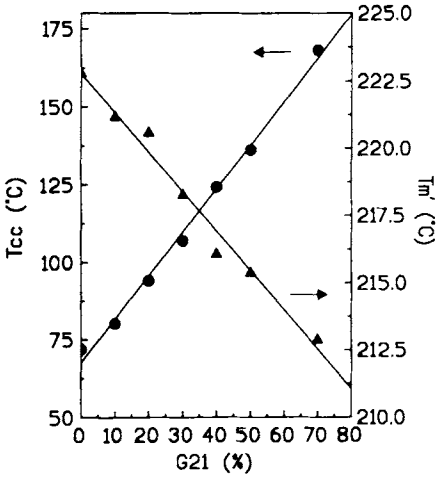

Figure 5 Cold-crystallization (T_{cc}) and melting (T'_m) temperatures for PA6/G21 blends.

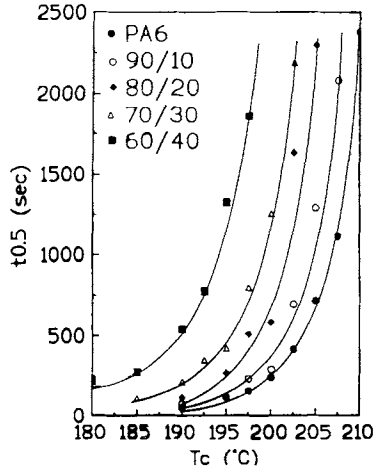

Figure 6 Half-time of crystallization ($t_{0.5}$) vs. crystallization temperature (T_c) for PA6/G21 blends.

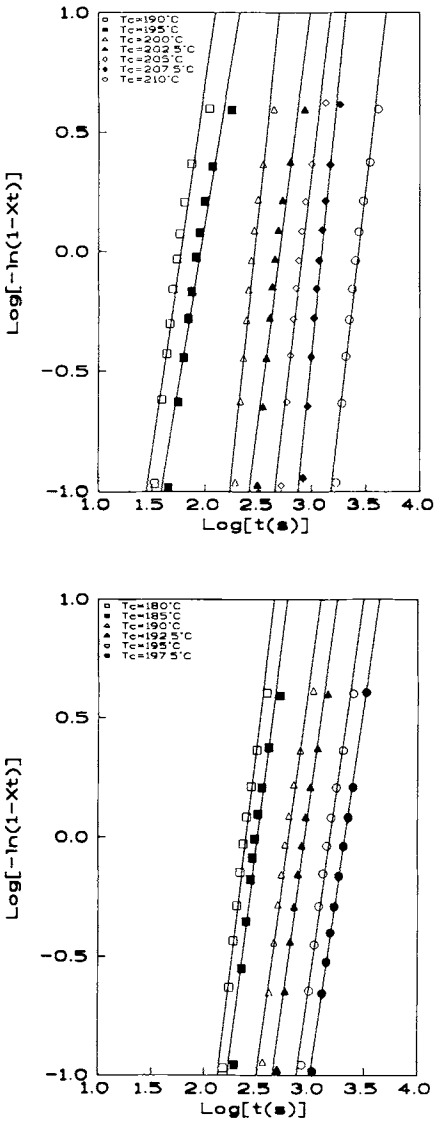

Figure 7 Avrami plots for (a) PA6 and (b) 60/40 blend.

position; the T_g for PA6 and G21 were found at 46 and 131.5°C, respectively. Although it is difficult to obtain completely amorphous nylon 6 by simple quench-cooling, our samples (after quenching) appeared amorphous by WAXS analysis and so any resulting influence of the eventual poor crystallinity on T_g has been considered insignificant. The appearance of a single T_g suggests that the mixture presents a single homogeneous amorphous phase, i.e., that the two components are miscible in the amorphous phase. In fact, the existence of only one composition-dependent glass transition temperature for a blend of two pure polymers is sufficient proof of polymer compatibility. With a miscible pair of polymers, the local molecular environment between

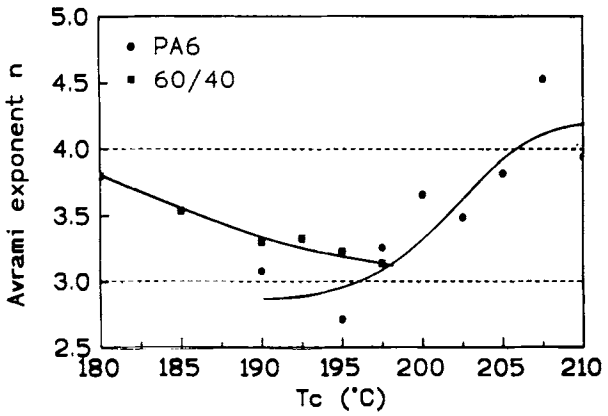

Figure 8 Avrami exponent (n) for PA6 and 60/40 blend.

polymer chains is the same as that of adjacent monomer units on the same chain.

The dependence of the T_g value on composition is shown in Figure 3, where the dotted curve is the trend of the theoretical Fox relation[14] and the solid line is the trend of the Gordon–Taylor equation,[15] which can be written as

$$T_g = (W_1 \cdot T_{g1} + k \cdot W_2 \cdot T_{g2})/(W_1 + k \cdot W_2)$$

where T_g, T_{g1}, and T_{g2} are the glass transitions of the blend and of the two plain components, W_1 and W_2 are the weight fractions, and k is an adjusting parameter related to the degree of curvature of the T_g-composition diagram and it can be considered as a measure of the molecular degree of mixing of two polymers in a blend. If k equals unity, a straight line is found.[16] For these blends, k was determined to be 0.67, indicating a good degree of mixing.

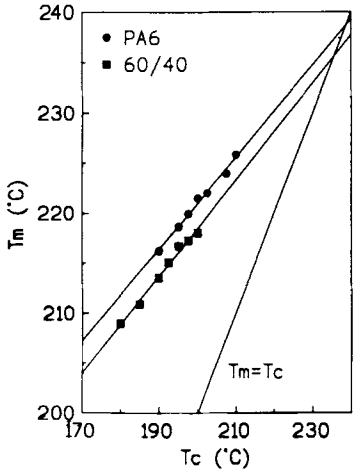

Figure 9 Observed melting temperatures (T_m) vs. T_c for PA6 and 60/40 blend.

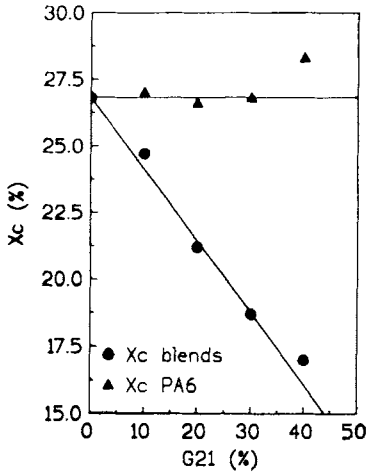

Figure 10 Crystallinity values at T_c = 190°C for PA6 (X_{cPA6}) and blends (X_{cblend}).

Continued heating of the quench-cooled blends above their respective T_g induced crystallization of the PA6 component and its subsequent melting (Fig. 4). The T_{cc} and T'_m values were found composition-dependent (Fig. 5).

The linear increase of T_{cc} vs. G21 content provides a qualitative confirmation of a reduction of the crystallization rate. The decrease of the T'_m, together with higher glass transition temperatures, leads to improved values of the T_g/T'_m ratio (0.75 for a 30/70 blend) compared to the value found for the PA6 (0.65). This is expected for polymers miscible in the melt, where the amorphous component of higher T_g hinders the crystallization; an analogous trend was observed for random copolymers.[17]

Isothermal Crystallization Kinetics

The half-time of crystallization obtained from the isotherm of crystallization is plotted in Figure 6 as a function of T_c for the PA6/G21 blends. The trend of these curves indicates that the addition of G21 to PA6 causes a reduction in the overall crystallization rate. Figure 7 shows plots of $\log[-\ln(1 - X_t)]$ against $\log t$ for PA6 and the 60/40 blend in the linear trend obtained until a high degree of conversion.

Several investigations have been carried out on the crystallization process of PA6 and most of the published data have been interpreted by means of the Avrami equation. It was found that the value of n depends on crystallization temperature,[18,19] molecular weight,[20] and nucleating agents.[21]

Figure 8 shows a plot of the obtained Avrami index n vs. T_c for PA6 and the 60/40 blend; n values for the 90/10, 80/20, and 70/30 are scattered between 3 and 4.5 and their trend is not significant. A similar trend of n vs. T_c for PA6 was previously reported[18,19]

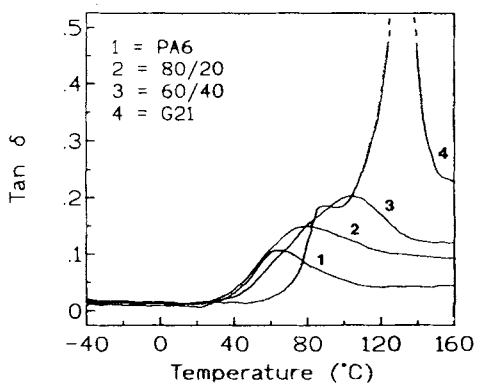

Figure 11 Loss factor (tan δ) for pure polymers and blends.

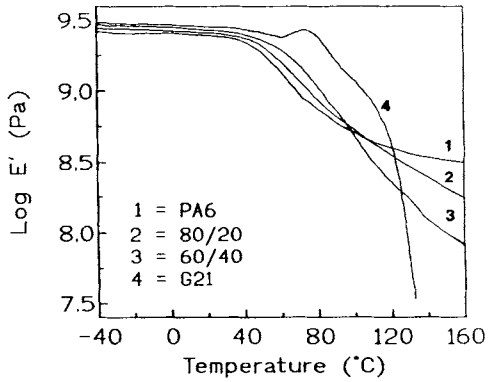

Figure 12 Storage moduli (E') for pure polymers and blends.

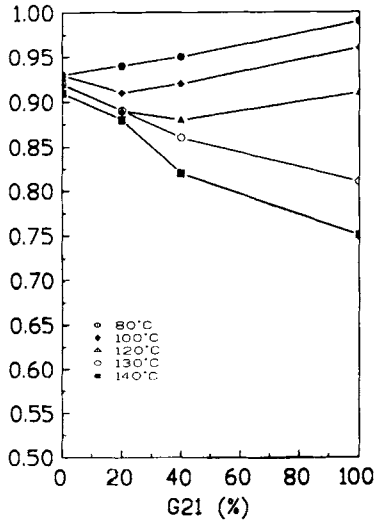

Figure 13 Modulus-maintaining ratio vs. G21 content at different temperatures.

Table I Tensile Mechanical Properties for Pure Polymers and Blends

PA6/G21	E (MPa)	σ_y (MPa)	ε_y (%)	σ_r (MPa)	ε_r (%)
100/0	560 ± 55.5	33.0 ± 2.1	24.0 ± 1.5	50 ± 4.2	240 ± 36.6
90/10	840 ± 69.1	34.9 ± 2.7	14.7 ± 2.2	46 ± 2.9	175 ± 25.5
80/20	1100 ± 97.8	44.0 ± 2.9	9.5 ± 1.2	41 ± 4.0	29 ± 6.1
70/30	1390 ± 110.8	50.7 ± 3.3	6.8 ± 0.6	41 ± 4.9	17 ± 3.2
60/40	1410 ± 97.4	52.4 ± 3.0	6.3 ± 0.6	40 ± 2.9	8 ± 1.8
0/100	2240 ± 178.0	71.0 ± 4.5	5.4 ± 0.4	39 ± 3.9	7 ± 1.5

and accounted for thermal heterogeneous nucleation followed by spherulitic growth.

The apparent melting point values linearly increase with the crystallization temperature for plain PA6 and for the blends (Fig. 9). The equilibrium melting point (T_m^0) of PA6 was estimated to be 237°C, a value in good accordance with previous findings.[11] For the 60/40 blend, a T_m^0 value of 235°C was calculated, while for the other blends, it was not possible to obtain a revealing estimate of T_m^0.

Both PA6 and its blends showed that only for $T_c \geq 200$°C was it possible to observe a single melting endotherm, but the melting behavior was quite sensitive to the heating rate, and at a scan rate of 20°C/min, only one endotherm was produced even for $T_c = 180$°C. The sensitivity of the melting behavior to heating rate could indicate the influence of morphological factors on the T_m[22], but, although the Hoffman–Weeks plots of T_m vs. T_c (Fig. 9) were linear, it is difficult to state that their slope, related to morphology, was independent of blend composition.

Thus, the melting point depression may be assigned to either a kinetic or a thermodynamic effect, but, if only the latter is considered, the Flory's interaction parameter will be very small for PA6/G21 blends, resulting from a small T_m depression.[22] Further studies are in progress to evaluate the relative importance of the thermodynamic effects vs. the morphological ones.

The values of $X_{c\text{PA6}}$ and $X_{c\text{blend}}$ ($T_c = 190$°C) are plotted vs. composition in Figure 10 and it emerges that PA6 crystallizes to the same extent as that in the pure state. This behavior is unusual, although annealing and morphological effects, dependent on composition and time, must be taken into account.

Dynamic Mechanical Behavior

The loss factors as a function of temperature for pure polymers and 80/20 and 60/40 blends are reported in Figure 11. The tan δ curve of G21 shows a pick with a maximum at 131°C associable with the glass to rubber transition, related to the onset of main chain segmental motion, and a second relaxation, ranging from about 80 to 100°C that has not been assigned, but it is tentatively associable with some restricted motion of the main chain. PA6 shows the glass-to-rubber transition at 62°C and the blends exhibit a single transition at a temperature intermediate between those of the two components; the peak temperature and the peak width tend to increase, increasing the G21 content. The presence of a single tan δ peak in the mechanical spectra of the blends suggests that, after crystallization of PA6, G21 forms a homogeneous amorphous phase with the noncrystallizable fraction of PA6. The increase in tan δ peak temperature, observed when the G21 content increases, indicates that the addition of G21 causes a shift to higher temperature of the glass transition temperature.

At the glass transition temperature, PA6 shows a modest E' drop due to the presence of a conspicuous crystalline fraction; on the contrary, G21, due to its amorphous nature, presents a marked decrease of E' (Fig. 12) after the glass transition. In agreement with the tan δ trend, the E' values of blends begin to decrease at temperatures higher than that for PA6, and up to about 100°C, the E' value for the blends is higher than that of PA6. At higher temperatures, the E' trend for the blend at lower G21 content resembles that of PA6, while, as the G21 content increases, the modulus decreases more rapidly, becoming similar to the behavior of amorphous G21.

The extent of lowering of the storage modulus with increasing temperature can be expressed by the modulus-maintaining ratio, i.e., the ratio of the modulus at a particular temperature and its constant value at a lower temperature (Fig. 13). At 80°C, the modulus-maintaining ratio increases with G21 content, while at higher temperatures, it progressively tends to decrease. This is because there are two phases in the blends: one is the miscible amorphous phase and the other is the PA6 crystalline one. When the temperature is below the T_g of G21, this com-

ponent can maintain very good mechanical properties, and since the T_g of the miscible amorphous phase increases with G21 content, the modulus-maintaining ratio also increases as a result of this. When the temperature is higher than the T_g of G21, the modulus of the amorphous phase shows a large decrease and therefore the crystalline PA6 is the main factor affecting the modulus of the blends. Since the crystallinity of the blends decreases with increasing G21 content, the modulus-maintaining ratio also decreases.

Tensile Mechanical Properties

The tensile mechanical properties of pure polymers and blends are reported in Table I. A stiffener action of G21 is evident; in fact, E and σ_y increase, increasing the G21 content, while a decrease of ε_y and σ_r is observable. The σ_r values of the blends decrease, increasing the G21 content because G21 has a lower strength than has PA6. The stiffener effect can be accounted for considering that the increase in T_g of the blends, which means a reduction in molecular mobility, causes the chains to flow more difficultly.

CONCLUSIONS

The presence of a single amorphous phase in quenched blends and the effect of G21 on the crystallization and melting behavior of PA6 seem to indicate the existence of a high degree of compatibility between the two components. The dynamic mechanical behavior of PA6/G21 blends suggests the presence of a single amorphous phase in crystallized samples of blends, and tensile mechanical tests indicate that G21 acts as a stiffener of PA6. These data are in accordance with the thermal behavior and confirm the hypothesis of compatibility between PA6 and G21. Investigations about gas barrier properties and the phase structure of PA6/G21 blends are in progress.

This work was partly supported by the "Progetto Finalizzato Chimica Fine II" of the Italian CNR. The authors thank Dr. P. Buzio for his useful suggestions and Dr. L. Zetta for the NMR investigations.

REFERENCES

1. R. J. Hernandez, J. R. Giacin, and E. A. Grulcke, *J. Membr. Sci.*, **65,** 187 (1992).
2. S. Nagaraj, R. J. Hernandez, and J. Giacin, in *Proceedings of the "7th World Conference on Packaging,"* Jaabeurs, Holland, April 14–17, 1991.
3. T. S. Ellis, *Polymer,* **29,** 2015 (1988).
4. T. S. Ellis, *Macromolecules,* **22,** 742 (1989).
5. T. S. Ellis, *Macromolecules,* **23,** 1494 (1990).
6. T. S. Ellis, *Polymer,* **31,** 1058 (1990).
7. T. S. Ellis, *Polym. Eng. Sci.,* **30,** 998 (1990).
8. T. S. Ellis, *J. Appl. Polym. Sci.,* **36,** 451 (1988).
9. D. R. Paul and J. S. Barlow, *Polymer,* **25,** 487 (1984).
10. J. H. Margill, *J. Appl. Phys.,* **35,** 3249 (1964); *J. Polym. Sci. A-2,* **5,** 89 (1967).
11. M. Avrami, *J. Chem. Phys.,* **7,** 1103 (1939).
12. B. Wunderlich, *Macromolecular Physics,* Academic Press, New York, 1980, Vol. 3.
13. L. Mandelkern, *Crystallization of Polymers,* McGraw-Hill, New York, 1982.
14. T. G. Fox, *Bull. Am. Phys. Soc.,* **2,** 123 (1956).
15. M. Gordon and J. S. Taylor, *J. Appl. Chem.,* **2,** 493 (1952).
16. G. Belorgey, M. Aubin, and R. Prud'homme, *Polymer,* **23,** 1051 (1982).
17. D. W. Van Krevelen, *Properties of Polymers,* Elsevier, Amsterdam, 1972.
18. M. Inoue, *J. Polym. Sci.,* **55,** 753 (1961).
19. E. Turska and S. Gogolewski, *Polymer,* **12,** 617 (1971).
20. E. Turska and S. Gogolewski, *Polymer,* **12,** 629 (1971).
21. G. Gurato, D. Gaidano, and R. Zannetti, *Makromol. Chem.,* **179,** 231 (1978).
22. T. Nishi and T. T. Wang, *Macromolecules,* **8,** 909 (1975).

Received December 16, 1994
Accepted November 7, 1995